

STUDY OF PHYSICAL PROCESSES CREATED BY SAND GRAINS IN THE WORKING NODES OF ADJUSTABLE THROTTLE

J.N. Aslanov¹ T.U. Khankishiyeva² L.T. Huseynova²

1. Industrial Machines Department, Azerbaijan State Oil and Industry University, Baku, Azerbaijan, tribo72@mail.ru

2. Industrial Machines Department, Azerbaijan State Oil and Industry University, Baku, Azerbaijan
tamilla.khankishiyeva72@mail.ru, lemanbabaxanova@mail.ru

Abstract- An adjustable throttle is installed on the flow line of a christmas tree of oil well and designed to regulate its operating mode. Regulation of the operating mode of a flowing well is required in cases where its wellhead pressure for this reason deviates from its permissible value, while this deviation can occur in the direction of increase or decrease. In sand-producing flowing oil wells, when the passage parts (valve and seat) of an adjustable throttle are corroded, the wellhead pressure of the well drops. Also, when the throttle passage is clogged, it rises, that is, in both cases, the operating mode of the flowing well is violated. The work of an adjustable throttle of a flowing oil well has been investigated and a method for calculating the resulting normally acting components of pressure forces on the surface of a spherical sand particle has been proposed. The spherical surface of a sand particle in its upper half is divided into nine parts of different sizes by intersecting with 9 secant horizontal parallel planes. The first part is the lateral surface of the spherical segment. The other eight parts are the side surfaces of various spherical plastics. First, the areas of the lateral surfaces of all the obtained parts of the hemispherical surface have been calculated, then - the vertical components of the pressure force on these parts. The sum of all these vertical distributed pressure forces is 2.00423 H for one sand particle, and for 32 particles it will be 60.1269 N. In addition, the value of the gravity of one sand particle has been determined, which is $1.3851 \cdot 10^{-3} \text{N}$ and for 32 particles - $44.208384 \cdot 10^{-3} \text{N}$. The above results allow to choose much more compatible materials for valve construction in order to increase its durability by determining the advanced force that sand grains can create. By identification of maximum force created by sand grains in the unit in sand wells, it will be possible to define the thrusts created by sand grains inside throttle. Once the material has been chosen based on maximum value of thrust, it will be resistant to hydro-abrasive wear.

Keywords: Adjustable Throttle, Flowing Well, Valve, Seat, Spherical Plastic, Wellhead Pressure.

1. INTRODUCTION

An adjustable throttle is installed on the flow line of christmas tree of oil-well and designed to regulate its operating mode. Regulation of the operating mode of a

flowing well is required in cases where its wellhead pressure for this reason deviates from its permissible value, while this deviation can occur in direction of increase or decrease.

In sand-producing flowing oil wells, when the passage parts (valve and seat) of an adjustable throttle are corroded, the wellhead pressure of the well drops. Also, when the throttle passage is clogged, it rises, that is, in both cases, the operating mode of the flowing well is violated. When the valve and the throttle seat are corroded, they are replaced with new ones, and when the throttle is clogged, using the flywheel, slightly rotating the stem, the valve is raised. With the expansion of the throttle section with a high-speed downflow, all mechanical impurities accumulated in the throttle rotate, as a result of which the throttle is cleaned. After that, the valve is returned to its optimal position [1-4].

2. METHODS FOR SOLVING STATED PROBLEM

The throttles, which are the main part of the Christmas tree used in oil and gas industry, are the main equipment used to adjust the regime parameters of the fountain well. Increasing the durability of such a controlling unit depends on reliability of its regulatory part. Studies have shown that sand particles in the oil and gas mixture cause the valve regulatory details to be corroded and consequently lead to a failure. Wear amount depends on the diameter of sand grains in well product and working pressure of the fluid. Sand grains movement under pressure lead to fret the packing elements of the valve and consequently get the material exhausted which led to the wearing and failure of the construction. Figuring out the force created by the sand grains, it is possible to identify thrust force accordingly. Advanced determination of the tip and saddle materials strength that are resistant to thrusts will increase the durability of overall construction. The purpose of current research paper is therefore aimed to determine the dependence of thrust from sand grains diameters.

In most cases, a special change in the operating mode of a flowing oil well is required when investigating them for inflow in steady flow regimes, that is, when taking indicator diagrams. Such studies are carried out in order to establish the optimal technological mode of operation, even in non-sand-flowing wells [5-8].

The most efficient unit of the regulated throttle is the "valve-seat" pair, since the parts of this pair are corroded by particles of sand and other rocks are eroded by acids and salts of striatal wastewater. In Figure 1, a plug assembly of an adjustable flow control throttle is shown.

The composition of the product of a sand-producing oil flowing well contains particles of sand and other hard rocks of various sizes and shapes. When an adjustable throttle is used in such wells, the study of their work is complicated, therefore, to simplify the solution of this problem, the following omissions are made [9]:

- The shape of the sand particles is accepted as spherical, moreover, their largest diameter is $d = 1$ mm;
- Also sand particles in the composition of products make up the majority;
- The diameter of the remaining sand particles is $d < 1$ mm; they pass freely through the throttle;
- The width of the annular gap in the passage of the adjustable throttle is close to 1 millimeter when the flowing well is operating in the optimal technological mode of operation. Therefore, the sand particles are caught and remain there in the first row and they are arranged as in Figure 1, there are 32 of them;
- After the formation of the first row of sand particles, the second row is collected on it, then the third, fourth, etc., rows of sand particles of the same diameter are collected on each other, form a fictitious porous medium.

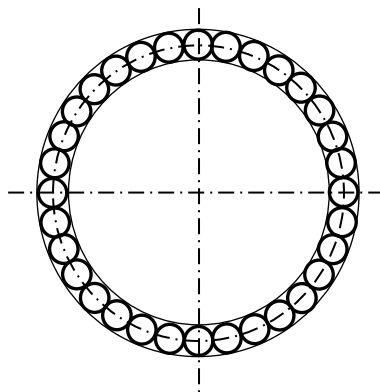


Figure 1. Arrangement of spheres in the annular gap of the valve with adjustable throttle

For a correct study of the operation of an adjustable throttle of a flowing well, it is necessary to know some of the features of a fictitious porous medium and a material of quartz sand [1-3].

3. METHODS

Let's use the following formula to determine the pore ratio of an imaginary porous medium using simple geometric hypotheses [10, 15]:

$$m = 1 - \frac{\pi}{6(1 - \cos \alpha) \sqrt{1 + 2 \cos \alpha}} \quad (1)$$

where, α is the acute angle of the rhombus that makes up the main face of the rhombohedron.

This angle characterizes the order of the eight elements of the fictitious rock and varies from 60° (the most dense arrangement) to 90° (the least dense arrangement).

At $\alpha = 60^\circ$; $m = 0.250$.

At $\alpha = 90^\circ$; $m = 0.476$ that is, in the range of $60^\circ \ll \alpha < 90^\circ$, the range of change in the porosity of the fictitious group is $0.25 \ll m < 0.476$.

In Figure 2, different schemes of two extreme positions of eight spherical sand particles of the same diameter are shown.

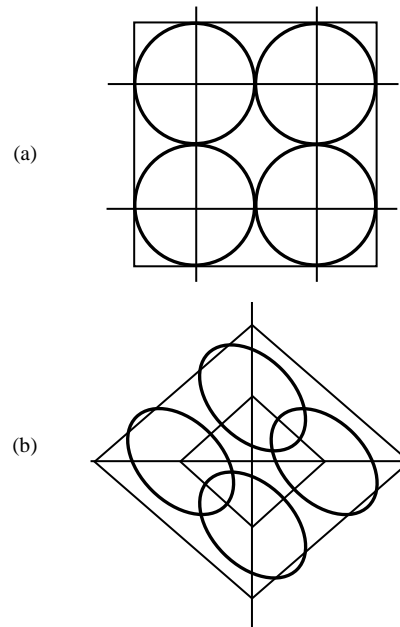


Figure 2. Location of sand grain according to Ch. Slikhter: (a) $\alpha=90^\circ$, (b) $\alpha=60^\circ$

Table 1. Mohs hardness of minerals

Mohs hardness	Reference mineral	Absolute hardness	Workability	Other minerals with similar hardness
1	Talc	1	Scratched with a fingernail	Graphite
2	Gypsum	3	Scratched with a fingernail	Halite, chlorite
3	Calcite	9	Scratched with copper	Biotite, gold, silver
4	Fluorite	21	Easily scratched with a knife, window glass	Dolomite, sphalerite
5	Apatite	48	Scratched with effort with a knife, window glass	Hematite, lapis lazuli
6	Orthoclase	72	Scratches glass. File processed	Opal, rutile
7	Quartz	100	Amenable to diamond processing, scratches glass	Garnet, tourmaline
8	Topaz	200	Amenable to diamond processing, scratches glass	Beryl, spinel
9	Corundum	400	Amenable to diamond processing, scratches glass	Sapphire, ruby
10	Diamond	1600	Cuts glass	Elbor

The material of sand particle is composed of a quartz mineral called silicium oxide (SiO). This mineral is too strong and resistant to compression deformation. Table 1 shows the hardness of minerals on the Mohs scale.

Table 1 consists of a row of 10 minerals of varying hardness, arranged in series from the most fragile mineral to the hardest mineral: Talc, Halite, Calcite, Fluorite, Apatite, feldspar, Quartz, Corundum, Topaz, Diamond.

The softest mineral is Talc and the hardest one is Diamond. Table 1 shows that quartz ranks seventh and is among the four hard minerals [2, 11, 13]. In Table 1 each subsequent mineral damages the previous mineral during their joint friction [2, 12, 14].

In order to study the operation of an adjustable throttle of a flowing well, it is necessary to determine the forces of the wellhead pressure acting on a spherical particle of sand and consider the equilibrium condition for these forces. And for this, in turn, the values of the geometric values of the sphere and its subsequent elements are calculated. The surface area of a sphere is calculated using the following formula:

$$S = 4\pi R^2 = \pi D^2 \quad (2)$$

The volume of the sphere is determined by the formula:

$$V = \frac{4}{3}\pi R^3 = \frac{1}{6}\pi D^3 \quad (3)$$

The part separated from the sphere by the secant is called the sphere segment. In Figure 3, a diagram of the spherical segment is given: where R is the radius of the circle; h is the height of the spherical segment, O is the center of it, and A is the radius of the base of the segment.

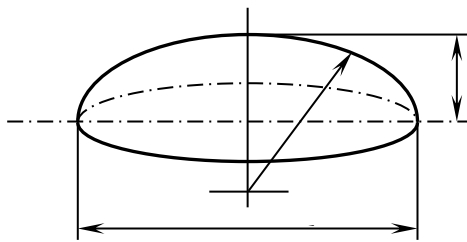


Figure 3. Diagram of the spherical segment

From Figure 3 the following relationship has been found:

$$a^2 = h(2R - h)$$

from here we get:

$$a = \sqrt{h(2R - h)} \quad (4)$$

The lateral surface area of the sphere element is determined by the following formula:

$$M = 2\pi Rh = \pi(a^2 + h^2) \quad (5)$$

The total surface area of a spherical segment is equal to the sum of its lateral surface area and the area of its circular base and is calculated by the following formula:

$$S = \pi(2Rh + a^2) = \pi(h^2 + 2a^2) \quad (6)$$

The volume of the spherical segment is calculated using the following formula:

$$V = \frac{1}{6}\pi h(3a^2 + h^2) = \frac{1}{3}\pi h^2(3R - h) \quad (7)$$

Equation (7) determines that the volume of a segment depends on its height and the radius of the circle. To calculate the values of the pressure forces acting on the

surface of a spherical sand particle, it is also required to determine the area of the lateral surface of the spherical plastics.

The intersection of a sphere with two parallel planes forms a spherical plastic. To determine the area of the lateral surface of a spherical plastic, a separate formula is not required, since the value of this quantity can be calculated with (5) for two adjacent spherical segments; here the difference in the areas of their lateral surfaces is considered. In Figure 4, a design scheme for calculating all pressure forces on one particle of spherical sand, on which all pressure forces are applied have been presented.

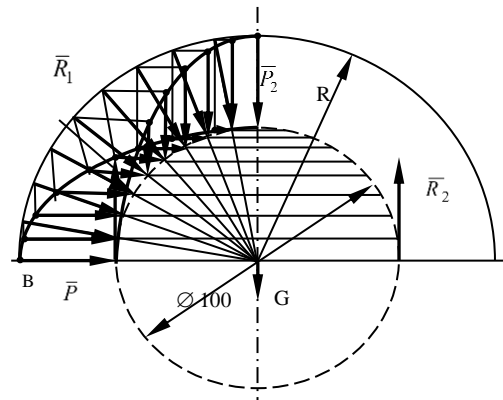


Figure 4. Diagram of the distribution of pressure forces acting normally on the surface of a spherical sand particle (Scale 100:1)

From Figure 4 it can be seen that points 1, 2, 3, ..., 10 taken on the lateral surface of the hemisphere have been built using a 10° central node. At each of these 10 points, the pressure vector B is applied to the surface of the sphere everywhere in the normal direction (according to Pascal's law); moreover, the directions of action of these vectors pass through the center "O" of the sphere.

From points 2, 3, 4, ..., 9, eight pieces of secant horizontal planes have been drawn, and as a result, nine pieces of spherical segments and eight pieces of spherical steam plastics have been obtained (mm²).

First, we calculate their lateral surface areas. The lateral surface area of the second smallest spherical segment will be:

$$M_I = 2\pi Rh = 2 \times 3.14 \times 0.5 \times 0.01 = 0.0314 \text{ mm}^2.$$

The lateral surface area of the II-th spherical segment will be: $M_{II} = 2 \times 3.14 \times 0.5 \times 0.01 = 0.0942 \text{ mm}^2$.

The lateral surface area of the 1st spherical plastic will be: $M_{I.s.p.} = M_{II} - M_I = 0.0942 - 0.0314 = 0.0628 \text{ mm}^2$.

The lateral surface area of the III spherical segment will be: $M_{III} = 2 \times 3.14 \times 0.5 \times 0.07 = 0.2198 \text{ mm}^2$.

The lateral surface area of the II spherical plastic will be: $M_{II.s.p.} = M_{III} - M_{II} = 0.2198 - 0.0942 = 0.1256 \text{ mm}^2$.

The lateral surface area of the IV spherical segment will be: $M_{IV} = 2 \times 3.14 \times 0.5 \times 0.125 = 0.3925 \text{ mm}^2$.

The lateral surface area of the III spherical plastic will be: $M_{III.s.p.} = M_{IV} - M_{III} = 0.3925 - 0.2198 = 0.1727 \text{ mm}^2$.

The lateral surface area of the V-th spherical segment will be: $M_V = 2 \times 3.14 \times 0.5 \times 0.17 = 0.5338 \text{ mm}^2$.

The lateral surface area of the IV spherical plastic will be: $M_{IV_{s.p.}} = M_V - M_{IV} = 0.5338 - 0.3925 = 0.1413 \text{ mm}^2$.

The lateral surface area of the VI-th spherical segment will be: $M_{VI} = 2 \times 3.14 \times 0.5 \times 0.25 = 0.7850 \text{ mm}^2$.

The lateral surface area of the V-th spherical plastic will be: $M_{V_{s.p.}} = M_{VI} - M_V = 0.7850 - 0.5338 = 0.1912 \text{ mm}^2$.

The lateral surface area of the VII-th spherical segment will be: $M_{VII} = 2 \times 3.14 \times 0.5 \times 0.315 = 0.9891 \text{ mm}^2$.

The lateral surface area of the VI spherical plastic will be: $M_{VI_{s.p.}} = M_{VII} - M_{VI} = 0.9891 - 0.7850 = 0.2041 \text{ mm}^2$.

The lateral surface area of the VIII-th spherical segment will be: $M_{VIII} = 2 \times 3.14 \times 0.5 \times 0.41 = 1.2874 \text{ mm}^2$.

The lateral surface area of the VII spherical plastic will be: $M_{VII_{s.p.}} = M_{VIII} - M_{VII} = 1.2874 - 0.9891 = 0.2983 \text{ mm}^2$.

The lateral surface area of the IX spherical segment (half of sphere) will be: $M_{IX} = 2 \times 3.14 \times 0.5^2 = 1.5700 \text{ mm}^2$.

The lateral surface area of VIII (last) spherical plastic will be $M_{VIII_{s.p.}} = M_{IX} - M_{VIII} = 1.5700 - 1.2874 = 0.2826 \text{ mm}^2$.

As it is seen from Figure 4, all vectors of the wellhead pressure acting normally on the spherical surface of the sand particle are divided into components, some of which act in the vertical direction, others in the horizontal direction. The horizontal pressure components compress the sand particle onto the surface of the variable throttle valve, and the vertical pressure components push the sand particle downward. Suppose a flowing well is operating at its optimal technological mode and the wellhead pressure in front of an adjustable throttle is

$$P_a = 30aT = 3.0 \text{ MPa}$$

And now we calculate the values of the vertical components of the pressure forces. There is the following relationship between the wellhead pressure P_a and the pressure force F :

$$F = P_a \times M \tag{8}$$

This force vector F acts normally in parts of the hemispherical surface. The vertical component of this force is determined by the formula:

$$F_v = F \times \cos \alpha = P_a \times M \times \cos \alpha \tag{9}$$

First, we determine the vertical components of the pressure vector P_a . At point 1, the pressure vector P acts normally on the spherical surface, and also has a vertical position; that is: $\alpha = 0^\circ$. Therefore, we have:

$$P_{v_1} = P \times \cos \alpha = 3.0 \times \cos 0^\circ = 3.0 \times 1 = 3.0 \text{ MPa}$$

At point 2, we have:

$$P_{v_2} = 3.0 \times \cos 10^\circ = 3.0 \times 0.9848 = 2.954 \text{ MPa}$$

At point 3:

$$P_{v_3} = 3.0 \times \cos 20^\circ = 3.0 \times 0.9397 = 2.819 \text{ MPa}$$

At point 4:

$$P_{v_4} = 3.0 \times \cos 30^\circ = 3.0 \times 0.8660 = 2.598 \text{ MPa}$$

At point 5:

$$P_{v_5} = 3.0 \times \cos 40^\circ = 3.0 \times 0.7660 = 2.298 \text{ MPa}$$

At point 6:

$$P_{v_6} = 3.0 \times \cos 50^\circ = 3.0 \times 0.6428 = 1.928 \text{ MPa}$$

At point 7:

$$P_{v_7} = 3.0 \times \cos 60^\circ = 3.0 \times 0.5 = 1.5 \text{ MPa}$$

At point 8:

$$P_{v_8} = 3.0 \times \cos 70^\circ = 3.0 \times 0.3420 = 1.026 \text{ MPa}$$

At point 9:

$$P_{v_9} = 3.0 \times \cos 80^\circ = 3.0 \times 0.1736 = 1.521 \text{ MPa}$$

At point 10:

$$P_{v_{10}} = 3.0 \times \cos 90^\circ = 3.0 \times 0 = 0 \text{ MPa}$$

In Figure 4, the AC10 curve has been drawn through the end points of the vertical components of the pressure vectors P_a , and the BC1 curve has been drawn through the end points of the horizontal components of the pressure vectors P_a . As it can be seen, these two curves intersect at one point C at an angle $\alpha = 45^\circ$. And now we calculate the values of the resulting forces of the vertical components of the distributed pressure forces acting in the considered sections of the hemispherical surface. The smallest spherical segment is section I located at the top of the hemispherical surface. The acting net force of the distributed vertical components will be:

$$F_{b1} = \frac{P_1 + P_2}{2} \times M_I \times \cos \alpha_1 = \frac{30 + 29.54}{2} = 0.0314 \times 10^{-2} \times 0.9848 = 0.9193 \times 10^{-2} \text{ kq} = 0.09193 \text{ N}$$

In the I-th spherical plastic, it will be:

$$F_{b2} = \frac{P_2 + P_3}{2} \times M_{II} \times \cos \alpha_2 = \frac{29.54 + 28.19}{2} = 0.0942 \times 10^{-2} \times 0.9397 = 2.5551 \times 10^{-2} \text{ kq} = 0.025551 \text{ N}$$

In the II-th plastic, it will be:

$$F_{b3} = \frac{P_3 + P_4}{2} \times M_{III} \times \cos \alpha_3 = \frac{28.19 + 25.98}{2} = 0.2198 \times 10^{-2} \times 0.8660 = 5.1556 \times 10^{-2} \text{ kq} = 0.051556 \text{ N}$$

In III plastic, she will:

$$F_{b4} = \frac{P_4 + P_5}{2} \times M_{IV} \times \cos \alpha_4 = \frac{25.98 + 22.98}{2} = 0.3925 \times 10^{-2} \times 0.7660 = 7.36 \times 10^{-2} \text{ kq} = 0.0736 \text{ N}$$

In IV plastic, she will:

$$F_{b5} = \frac{P_5 + P_6}{2} \times M_V \times \cos \alpha_5 = \frac{22.98 + 19.28}{2} = 0.1912 \times 10^{-2} \times 0.6428 = 2.5969 \times 10^{-2} \text{ kq} = 0.25969 \text{ N}$$

In V plastic, it will:

$$F_{b6} = \frac{P_6 + P_7}{2} \times M_{VI} \times \cos \alpha_6 = \frac{19.28 + 15}{2} = 0.785 \times 10^{-2} \times 0.5 = 6.7275 \times 10^{-2} \text{ kq} = 0.67275 \text{ N}$$

In VI plastic, she will:

$$F_{b7} = \frac{P_7 + P_8}{2} \cdot M_{VII} \cdot \cos \alpha_7 = \frac{15 + 10.26}{2} = 0.2983 \times 10^{-2} \times 0.3420 = 1.2885 \times 10^{-2} \text{ kq} = 0.12885 \text{ N}$$

In the VII plastic, she will:

$$F_{b8} = \frac{P_8 + P_9}{2} \times M_{VIII} \times \cos \alpha_8 = \frac{10.26 + 5.21}{2} = 0.2826 \times 10^{-2} \times 0.173 = 0.379 \times 10^{-2} \text{ kq} = 0.0379 \text{ N}$$

Thus, the sum of all these vertical distributed pressure forces will be:

$$\sum_{i=1}^8 F_{b,i} = 0.9193 + 0.02555 + 0.051556 + 0.7360 + 0.25969 + 0.67275 + 0.12885 + 0.0379 = 2.00423 \text{ N}$$

In addition, this particle of sand is also acted upon by its gravity force, which is applied at the center of gravity of the particle and directed vertically downward; let's define its meaning. The specific gravity of the quartz sand material is:

$$\gamma_{kb} = 2.64 \frac{\text{q}}{\text{cm}^3} = 2.64 \times 10^6 \text{ N/m}^3$$

The volume of a spherical particle of sand with a diameter of 1 mm will be:

$$V = \frac{1}{6} \pi d^3 = \frac{1}{6} 3.14 \times (10^{-3})^3 = 0.5233 \times 10^{-9} \text{ m}^3$$

The weight of one sand particle will be:

$$G = V \gamma = 0.5233 \times 10^{-9} \times 2.64 \times 10^6 = 1.381512 \times 10^{-3} \text{ N} = 0.1381512 \text{ q}$$

and for 32 particles it will be 0.0442 N. Thus, the value of the total vertical force acting on the sand particle will be:

$$F_{sum} = \sum_{i=1}^8 F_{b,i} + G = 2.00423^{32} + 1.381512 \times 10^{-3} = 60.1269 + 0.0442 = 60.1711 \text{ N}$$

where, R_1 is the reaction force acting on the surface of the throttle valve, and R_2 is a similar force acting on the surface of the throttle valve seat. If we accept that: $R_1 = R_2 = R$, then we will have equilibrium Equation (11):

$$F_{sum} = 2R \tag{11}$$

From here, we get:

$$R = \frac{F_{sum}}{2} = \frac{60.1711}{2} = 30.086 \text{ N}$$

These reaction forces can be called resting frictional forces. From this, the following conclusion is obtained: wear of the parts of the throttle valve (the valve itself and the seat) is caused by the influence of these reaction forces.

4. ANALYSIS OF RESULTS

One of the main reasons for the failure of an adjustable flow control valve is abrasive erosion caused by spherical sand grains in the transported product. The mechanism of action of abrasive erosion depends on the pressure exerted by the sand grains. To find out the impact strength of abrasive erosion, it is necessary to determine the substitute for the pressure forces acting on the surface of a grain of sand in the normal direction. In the research work, a method for calculating the replacement of accumulations of pressure forces acting on the surface of a sand particle, acting in the normal direction has been proposed. To solve the problem, a technique is proposed in the following sequence.

- The shape of the sand particles is spherical, moreover, their largest diameter is $d = 1 \text{ mm}$;
- Also sand particles in the composition of products make up the majority;
- The diameter of the remaining sand particles is $d < 1 \text{ mm}$; they pass freely through the throttle;
- The width of the annular gap in the passage of the adjustable throttle is close to 1 millimeter when the flowing well is operating in the optimal technological mode of operation. Therefore, the sand particles are caught and remain in the first row and arranged as shown in Figure 1, there are 32 of them;
- After the formation of the first row of sand particles, the second row is collected on it, then the third, fourth, etc., rows of sand particles of the same diameter are collected on each other and form a fictitious porous medium. Simple geometric assumptions derived following equation for porosity coefficient of a fictitious porous medium:

$$m = 1 - \frac{\pi}{6(1 - \cos \alpha) \sqrt{1 + 2 \cos \alpha}}$$

where, α is the acute angle of the rhombus that makes up the main face of the rhombohedron. This angle characterizes the order of the eight elements of the fictitious rock and ranges from 60° (the most dense arrangement) to 90° (the least dense arrangement).

when, $\alpha = 60^\circ$; $m = 0.250$;

when, $\alpha = 90^\circ$; $m = 0.476$ that is, in the range of change $60^\circ, 60^\circ \ll \alpha \leq 90^\circ$, the range of change in the porosity of the fictitious group is: $0.25 \ll m \leq 0.476$.

This method has been proposed and allows to determine the shear force created by sand grains.

5. DISCUSSION

As a result, the spherical surface of a sand grain is divided into nine parts of different sizes using 9 secant parallel planes in its upper half; the first part is the lateral surface of the spherical segment, and the remaining eight parts are the half-surfaces of the various spherical layers.

First, the areas of the lateral surfaces of all parts of the resulting hemisphere surface have been calculated, and then - the vertical accumulations of compressive forces in these parts. The sum of all these vertically distributed compressive forces will be 2.0023 N for one sand particle and 60.1269 N for 32 particles.

In addition, the value of the weight of one particle of sand has been determined $1.38151 \times 10^{-3} \text{ N}$, and for 32 particles $44.208384 \times 10^{-3} \text{ N}$. Thus, the value of the substitute vertical force is obtained 104.34 N. In Figure 4, a design scheme is presented for calculating all pressure forces on one particle of spherical sand, on which all pressure forces are applied.

From Figure 4 it can be seen that points 1, 2, 3, ..., 10 taken on the lateral surface of the hemisphere have been built using a 10° central node. At each of these 10 points, the pressure vector B is applied to the surface of the sphere everywhere in the normal direction (according to Pascal's law); moreover, the directions of action of these vectors pass through the center "O" of the sphere.

From points 2, 3, 4, ..., 9, eight pieces of secant horizontal planes have been drawn, and as a result, nine pieces of spherical segments and eight pieces of spherical steam plastics have been obtained.

ACKNOWLEDGMENT

This work was financially supported by Science Development Foundation - Grant No. EIF-MQM-ETS-2020-1(35)-08/04/1-M-04.

7. CONCLUSIONS

The work of an adjustable throttle of a flowing well has been investigated and a method for calculating the resulting normally acting components of pressure forces on the surface of a spherical sand particle has been proposed.

The spherical surface of a sand particle in its upper half is divided into nine parts of different sizes by intersecting with 9 secant horizontal parallel planes. The first part is the lateral surface of the spherical segment. The other eight parts are the side surfaces of various spherical plastics.

The areas of the lateral surfaces of all the obtained parts of the hemispherical surface and the vertical components of the pressure force on these parts have been calculated; the sum of all these vertical distributed pressure forces was 2.00423 N. At 32 parts, it will be 60.1269 N. The value of the gravity of one sand particle is determined, which is 1.3851×10^{-3} N. After the throttle, the pressure of the liquid flow drops sharply and therefore, the action of the vertical components of pressure forces is not taken into account.

REFERENCES

[1] N. Engheta, R. Ziolkovski, "Metamaterials: Physics and Engineering Explorations", N.Y: John Wiley and Sons, 2006.
[2] Y. Zare, "1 Modeling Approach for Tensile Strength of Interphase Layers" Polymer Nanocomposites Journal of Colloid and Interface Science, Vol. 471, pp. 89-93, June 2016.
[3] I.M. Muravyov, M.N. Bazlov, A.I. Zhukov, B.S. Chernov, "Technology and Technology of Oil and Gas Production", Publishing House Nedra, pp. 206-217, Moscow, Russia, 1971.
[4] J.N. Aslanov, A.B. Sultanova, "Forecasting of Improved Straightforward Valves Technical Condition Using Fuzzy Inference Models", IFAC-Papers OnLine, Vol. 51, Issue 30, pp. 12-14, 2018.
[5] V.T. Mamedov, G.A. Mamedov, J.N. Aslanov, "Stress-Strain State of Reinforcing Rubber Membranes at Large Deformations", Journal of Applied Mechanics and Technical Physics, Vol. 61, No. 2, pp. 286-291, 2020.
[6] IUPAC, "Compendium of Chemical Terminology", The 2nd Ed., "Gold Book", (1997), Online Corrected Version: Shear Modulus, 2006.
[7] J.N. Aslanov, K.S. Mammadov, N.A. Zeynalov, "Selection Of Structural Materials For Improved Liner Motion Gate Valves Based On Friction Correlation Method", International Journal of Advanced Technology and Engineering Exploration this Link is Disabled, Vol. 9, No. 87, pp. 155-166, 2022.

[8] M. Babanli, "Theory and Practice of Material Development Under Imperfect Information", The 13th International Conference on Theory and Application of Fuzzy Systems and Soft Comp. (ICAFS), pp. 4-14, 2018.
[9] M. Babanli, R. Karimov, I.I. Abbasov, "An Impact of the Ladle Lining on the Refining of Reinforced Steel when Blowing with Powders", Eastern-European Journal of Enterprise Technologies, Vol. 5, No. 1, Issue 101, pp. 65-71, 2019.
[10] K.S. Basniev, A.M. Vlasov, I.N. Kochina, V.M. Maksimov, "Underground Hydraulics", Nedra, p. 303, Moscow, Russia, 1986.
[11] J.N. Aslanov, M.A. Ismailov, "Molecular Mutual Contact of Surfaces with the Highest Purity Class", Molodiy Vcheniy, No. 10, Issue 98, pp. 1-4, 2021.
[12] J.N. Aslanov, Z.S. Huseynli, N.M. Abbasov, A.V. Sharifova, "Durability Study of Specialized Sealing Elements", International Journal on Technical and Physical Problems of Engineering (IJTPE), Issue 52, Vol. 14, No. 3, pp. 8-13, September 2022.

BIOGRAPHIES



Name: Jamaladdin
Middle Name: Nuraddin
Surname: Aslanov
Birth day: 15.08.1972
Birth Place: Jalilabad, Azerbaijan
Bachelor: Mechanical Engineering,
Faculty of Oil Mechanical Engineering,

Azerbaijan State Oil Academy, Baku, Azerbaijan, 1995
Master: Mechanical Engineering, Faculty of Oil Mechanical Engineering, Azerbaijan State Oil Academy, Baku, Azerbaijan, 1997
Doctorate: Mechanical Engineering, Faculty of Oil Mechanical Engineering, Azerbaijan State Oil Academy, Baku, Azerbaijan, 2011
The Last Scientific Position: Assoc. Prof., Azerbaijan State Oil and Industry University, Baku, Azerbaijan, Since 2012
Research Interests: Valves, Tribological Research, Increase Friction and Wear Resistance of Units in Oil and Gas Fields Machinery and Equipment
Scientific Publications: 103 Papers, 2 Monograph, 2 Textbook, 4 Educational Supplies, 1 Methodological Resource, 8 Patents



Name: Tamila
Middle Name: Uzeyir
Surname: Khankishiyeva
Birth day: 01.08.1972
Birth Place: Baku, Azerbaijan
Bachelor: Mechanical Engineering,
Faculty of Oil Mechanical Engineering,

Azerbaijan State Oil Academy, Baku, Azerbaijan, 1994
Master: Mechanical Engineering, Faculty of Oil Mechanical Engineering, Azerbaijan State Oil Academy, Baku, Azerbaijan, 1996
Doctorate: Mechanical Engineering, Faculty of Oil Mechanical Engineering, Azerbaijan State Oil Academy, Baku, Azerbaijan, 2016

The Last Scientific Position: Assoc. Prof., Azerbaijan State Oil and Industry University, Baku, Azerbaijan, Since 2018

Research Interests: Well Rod Pump Unit, Technological Machines and Equipment, Tribological Research

Scientific Publications: 40 Papers, 4 Textbook, 4 Educational Supplies, 1 Methodological Resource



Name: **Laman**

Middle Name: **Telman**

Surname: **Huseynova**

Birthday: 14.06.1991

Birth Place: Baku, Azerbaijan

Bachelor: Engineering machinery and equipment, Faculty of Oil Mechanical Engineering, Azerbaijan State Oil Academy, Baku, Azerbaijan, 2014

Master: Engineering Machinery and Equipment, Faculty of Oil Mechanical Engineering, Azerbaijan State Oil Academy, Baku, Azerbaijan, 2016

Doctorate: Machinery, Equipment and Processes, Faculty of Oil Mechanical Engineering, Azerbaijan State Oil and Industry University, Baku, Azerbaijan, 2021

Research Interests: Adjustable Throttle, Wellhead Pressure, Increase the Efficiency of Throttles Being Used in Industry

Scientific Publications: 3 Papers, 1 Patent